Brief Communication

MOLECULAR METABOLISM

The incretin hormone GIP is upregulated in patients with atherosclerosis and stabilizes plaques in ApoE$^{-/-}$ mice by blocking monocyte/macrophage activation

Florian Kahles [1,3], Ana Liberman [1,3], Constantin Halim [1], Matthias Rau [1], Julia Möllmann [1], Robert Werner Mertens [1], Marcia Rückbeil [2], Irmgard Diepolder [1], Benedikt Walla [1], Sebastian Diebold [1], Mathias Burgmaier [1], Corinna Lebherz [1], Nikolaus Marx [1], Michael Lehrke [1,*]

ABSTRACT

Objective: The incretin hormones GLP-1 (glucagon-like peptide-1) and GIP (glucose-dependent insulinotropic peptide) are secreted by the gut after food intake leading to pancreatic insulin secretion and glucose lowering. Beyond its role in glucose control, GLP-1 was found in mice and men to beneficially modulate the process of atherosclerosis, which has been linked to improved cardiovascular outcome of patients with diabetes at high cardiovascular risk treated with GLP-1 receptor agonists. However, little is known on the role of the other main incretin in the cardiovascular system. The aim of this study was to characterize GIP in atherosclerotic cardiovascular disease.

Methods and results: Serum concentrations of GIP were assessed in 731 patients who presented for elective coronary angiography at the University Hospital Aachen. While GIP concentrations were not associated with coronary artery disease (CAD), we found 97 patients with PAD (peripheral artery disease) vs. 634 without PAD to have higher circulating GIP levels (413.0 $\pm$ 315.3 vs. 332.7 $\pm$ 292.5 pg/mL, $p = 0.0165$). GIP levels were independently related to PAD after multivariable adjustment for CAD, age, sex, BMI, hypertension, diabetes, CRP, WBC, and smoking. To investigate the functional relevance of elevated GIP levels in human atherosclerotic disease, we overexpressed GIP (1–42) in ApoE$^{-/-}$ mice fed a Western diet for 12 weeks using an adeno-associated viral vector system. GIP overexpression led to reduced atherosclerotic plaque macrophage infiltration and increased collagen content compared to control (LacZ) with no change in overall lesion size, suggesting improved plaque stability. Mechanistically, we found GIP treatment to reduce MCP-1-induced monocyte migration under In vitro conditions. Additionally, GIP prevented proinflammatory macrophage activation leading to reduced LPS-induced IL-6 secretion and inhibition of MMP-9 activity, which was attributable to GIP dependent inhibition of NfκB, JNK-, ERK, and p38 in endotoxin activated macrophages.

Conclusion: Elevated concentrations of the incretin hormone GIP are found in patients with atherosclerotic cardiovascular disease, while GIP treatment attenuates atherosclerotic plaque inflammation in mice and abrogates inflammatory macrophage activation in vitro. These observations identified GIP as a counterregulatory vasoprotective peptide, which might open new therapeutic avenues for the treatment of patients with high cardiovascular risk.

Keywords Incretin; GIP; Atherosclerosis; Plaque stability; PAD; Macrophages

1. INTRODUCTION

The two major incretin hormones GLP-1 (glucagon-like peptide-1) and GIP (glucose-dependent insulinotropic peptide) are secreted by enteroendocrine cells following nutrient intake leading to insulin secretion and glucose control [1]. This mode of action is currently used for the treatment of patients with type 2 diabetes [2]. Beyond its glucoregulatory role GLP-1 has been found to mediate various protective pleiotropic effects in different organ systems [3]. For example, we and others found GLP-1 to reduce and stabilize atherosclerotic lesions in ApoE$^{-/-}$ mice by directly blocking monocyte migration and preventing inflammatory activation of monocytes/macrophages [4, 5]. Two recent clinical trials (LEADER and SUSTAIN-6) showed improved cardiovascular outcomes in diabetic patients at high cardiovascular risk after treatment with the GLP-1-receptor agonists liraglutide and semaglutide on top of standard antidiabetic

[1]Department of Internal Medicine I-Cardiology, University Hospital Aachen, Pauwelsstraße 30, 52074 Aachen, Germany [2]Department of Medical Statistics, University Hospital Aachen, Pauwelsstraße 19, 52074 Aachen, Germany

[3] These authors contributed equally to this work.

*Corresponding author. Department of Internal Medicine I, University Hospital Aachen, Pauwelsstraße 30, D-52074 Aachen, Germany. Fax: +49 241 80 82545. E-mail: mlehrke@ukaachen.de (M. Lehrke).

Received March 26, 2018 • Revision received May 15, 2018 • Accepted May 17, 2018 • Available online 23 May 2018

https://doi.org/10.1016/j.molmet.2018.05.014

therapy [6, 7]. Interestingly, in both studies, GLP-1-receptor agonists reduced cardiovascular endpoints most likely through a reduction in atherosclerosis-related events. However, the role of the other main incretin hormone, GIP, in the cardiovascular system, beyond its insulinotropic function, is still largely unknown. Experimental work by Nagashima et al. demonstrated that infusion of GIP into non-diabetic ApoE$^{-/-}$ mice on an atherogenic diet for 4 weeks was able to reduce lesion size [8]. A study by Nogi and colleagues could reproduce the anti-atherosclerotic effects of GIP also in diabetic ApoE$^{-/-}$ mice [9], which was mechanistically linked to a reduction of plaque macrophages and direct GIP-receptor-mediated inhibition of foam cell formation. However, evidence is lacking on the effects of GIP on composition and stability of atherosclerotic plaques. Experimental and clinical imaging studies identified atherosclerotic plaques of patients with diabetes compared to non-diabetic patients to be more instable due to a thin fibrous cap and less collagen content with high amounts of proinflammatory macrophages, thus leading to high susceptibility of early plaque rupture and life threatening cardiovascular complications like consecutive myocardial infarction [10, 11]. Therefore, identifying new approaches to target plaque morphology and stability is of particular importance to improve cardiovascular outcomes in patients with diabetes. Here we investigated the role of GIP in atherosclerotic cardiovascular disease with a focus on plaque morphology.

2. METHODS

2.1. Clinical study

We analyzed blood samples from 731 patients in our cardiovascular biobank (542 male and 189 female); these patients underwent elective coronary angiography at the University Hospital Aachen (Department of Cardiology). Stable coronary artery disease (CAD) was present in 474 patients, and PAD (peripheral artery disease) was present in 97 patients, as presented in Table 1. Blood was collected in a random nonfasting manner. After centrifugation at 2,000 g at 4 °C for 20 min, serum aliquots of 1 mL were frozen immediately at −80 °C. Total GIP serum levels were determined by using a commercial ELISA kit (Millipore) according to the manufacturers' instructions. Study protocols and biosampling were approved by the local ethics committee and conducted in accordance with the ethical standards laid down in the 1964 Declaration of Helsinki (ethics committee of the University Hospital Aachen, RWTH Aachen University).

2.2. Experimental study

Recombinant adeno-associated viral constructs: Vectors carried transgene cassettes encoding b-galactosidase (LacZ) as control or GIP (1—42) under control of a cytomegalovirus (CMV) promoter. The pseudotyping strategy was used to generate AAV vectors encapsidated in an AAV8 capsid (AAV2.8) as previously reported [4, 12]. Successful vector cloning was proved by sequencing and restriction digests. Vectors were purified by standard cesium sedimentation. Titers were determined via Taq-Man RealTime polymerase chain reaction (PCR).

Animals: C57BL/6 ApoE$^{-/-}$ mice were purchased from Taconic, USA. Six-week-old male mice were housed under specific pathogen—free conditions in either individually ventilated or filter top cages with a 12-h light/12-h dark cycle with free access to autoclaved water and regular chow diet ad libitum. Mice were i.v. injected with AAV vectors via tail vein (LacZ vs. GIP 1—42; 5×10^{12} particles/mouse). Mice were switched to a western diet (39 kJ% fat, 41 kJ% carbohydrates and 20 kJ% protein (ssniff EF R/M acc. TD88137AQ8 mod.; ssniff Spezialdiäten GmbH, Germany) 4 weeks after i.v. vector injection on which they remained for a total of 12 weeks. Body weight was monitored

Table 1 — Baseline characteristics and GIP measurements.

Parameter	All patients	PAD (no)	PAD (yes)	No CAD	PAD (no)	PAD (no)	Stable CAD	PAD (no)	PAD (yes)
n	731	634	97	257	242	15	474	392	82
Age	65.3 ± 13.2[a]	64.5 ± 13.4	70.3 ± 10.2	60.6 ± 15.8	60.3 ± 15.8	65.8 ± 15.7	67.9 ± 10.7	67.2 ± 11.0	71.2 ± 8.8
BMI	28.3 ± 5.6[b]	28.3 ± 5.7	28.2 ± 4.9	28.6 ± 7.1	28.6 ± 7.2	27.8 ± 4.6	28.2 ± 4.6	28.2 ± 4.6	28.3 ± 5.0
Sex (male)	542 (74.3%)[c]	466 (73.7%)	76 (78.4%)	154 (60.4%)	146 (60.8%)	8 (53.3%)	388 (81.9%)	320 (81.6%)	68 (82.9%)
Hypertension	527 (72.2%)[a]	447 (70.5%)	80 (83.3%)	145 (56.6%)	137 (56.6%)	8 (57.1%)	382 (80.6%)	382 (80.6%)	72 (87.8%)
DM	239 (32.7%)	199 (31.4%)	40 (41.2%)	63 (24.5%)	61 (25.2%)	2 (13.3%)	176 (37.1%)	138 (35.2%)	38 (46.3%)
CRP	10.5 ± 16.7[d]	10.5 ± 17.4	10.1 ± 11.9	11.0 ± 16.9	11.0 ± 17.2	10.2 ± 10.4	10.2 ± 16.6	10.2 ± 17.5	10.0 ± 12.3
WBC	7.4 ± 2.5[e]	7.4 ± 2.5	7.2 ± 2.4	6.9 ± 2.1	7.0 ± 2.1	6.1 ± 1.5	7.6 ± 2.6	7.6 ± 2.7	7.4 ± 2.4
Smoker	289 (39.6%)[a]	235 (37.1%)	54 (56.3%)	89 (34.6%)	78 (32.2%)	11 (73.3%)	200 (42.3%)	157 (40.1%)	43 (53.1%)
GIP level	343.5 ± 296.7 (272.0, 73.1-545.6)[f]	332.7 ± 292.5 (258.4, 71.2-533.9)[1]	413.0 ± 315.3 (376.2, 118.2-624.5)[1]	370.7 ± 314.9 (310.8, 73.5-567.4)[2]	360.5 ± 310.4 (292.1, 71.0-551.0)[3]	531.6 ± 352.1 (475.0, 230.5-1008.2)[3]	328.9 ± 285.8 (252.9, 72.6-533.3)[2]	315.7 ± 280.1 (241.1, 71.2-519.5)[4]	391.2 ± 305.5 (368.1, 95.4-615.5)[4]

Continuous variables are expressed as mean ± SD and (median, Q1 − Q3) in case of skewed data. Categorical variables are shown as absolute and relative frequencies. [a] 1 missing value, [b] 12 missing values, [c] 2 missing values, [d] 118 missing values, [e] 92 missing values, [f] 11 missing values. [1] PAD vs. No PAD p-value = 0.0165, [2] CAD vs. No CAD pvalue= 0.1869, [3] No CAD: PAD vs. No PAD p-value = 0.0632, [4] Stable CAD: PAD vs. No PAD p-value = 0.0389.

weekly. We performed an oral glucose tolerance test (OGTT) after 10 weeks on Western diet following a 6 h fasting period. Blood glucose levels were measured with a glucometer (Contour, Bayer, Germany) at 0, 30, 60, 90, 120 min after oral glucose administration (2 g/kg body weight). After 12 weeks on Western diet, mice were anesthetized with Isoflurane (Abbott, Germany) and euthanized by cervical dislocation.

Serum lipid measurement: For quantification of serum cholesterol and triglycerides, the enzymatic CHOD-PAP method with diagnostic reagents for photometric systems (DiaSys Diagnostic, Germany) and photometer (TECAN, Switzerland) at 546 nm was used as described elsewhere [4].

Determination of circulating GIP levels: Blood was collected after a 6 h fasting period. Total GIP serum levels were determined by using a commercial ELISA kit (Millipore) according to the manufacturers' instructions.

Organ collection and processing: Aorta and heart were carefully perfused with PBS to remove blood residues. Cardiac apex was cut off and the aortic arch was separated from the aorta distal of the left subclavian artery, embedded in freezing medium (Tissue-Tek O.C.T. compound for cryo-sectioning, USA), and stored at 80 °C as previously described [4].

Atherosclerotic lesion assessment: To quantify plaque burden in the descending aorta, Oil-red-O staining was performed as previously described [4]. Briefly, fixed aortas were rinsed with PBS, washed in 100% propylene glycol and incubated for 20 min with Oil-red-O solution and counterstained in hematoxylin. By Oil-red-O staining of the aortic arch and the aortic root sections, plaque lipid content was determined. For visualization and measuring of plaque size in the aortic root and the aortic arch, hematoxylin staining was used. Atherosclerotic lesion size was determined by using Image Pro-Plus software (Media Cybernatics, USA).

Immunohistochemistry: To measure plaque macrophage content, acetone-fixed aortic root and aortic arch sections were stained with anti-mouse MOMA-2 antibody (AbD Serotecec, UK) using a biotinylated secondary antibody and hematoxylin and eosin for nuclear staining. Positive staining areas were selected by an investigator blinded to the treatment and analyzed by Image Pro-Plus software (Media Cybernatics, USA). For quantification of MMP-9 expression in the atherosclerotic plaques, we performed immunostaining using a specific MMP-9 antibody (Abcam, UK) as reported before [4]. To quantify collagen fiber content of the atherosclerotic plaques, formaldehyde-fixed sections of the aortic root and aortic arch were stained for 90 min in a 0.1% solution of Sirius Red in 1.2% picric acid solution as described previously [4, 13]. All sections were analyzed under a light microscope (Nikon, Tokyo, Japan).

Zymographies: To assess In vitro MMP-9 activity RAW 264.7 cells (ATCC, USA) (murine monocyte/macrophage cell line) were pretreated with GIP (1—42) (Bachem, Switzerland) at the indicated concentrations for 30 min and then stimulated with LPS (100 ng/mL). MMP-9 activity in the supernatant was measured by performing standard zymographies as previously described 72 h after LPS treatment [13].

Western blot analysis: Protein expression levels of MMP-9, phospho-JNK, JNK, phospho-ERK, ERK, phospho-p38, and p38 were determined by western blotting using specific antibodies as described previously [14]. RAW 264.7 cells were harvested in cell lysis buffer (Cell Signaling) and whole cell proteins were subjected to immunoblotting using the indicated antibodies (Cell Signaling).

IL-6 ELISA: Supernatant from RAW 264.7 cells was collected 24 h after LPS stimulation (100 ng/mL) and pretreatment for 30 min with GIP at the indicated concentrations. IL-6 levels were determined by using a commercial ELISA kit (R&D systems, MN, USA) according to the manufacturers' instructions.

NFκB activation assay: NFκB activation was measured in RAW 264.7 cells after pretreatment for 30 min with 1 nM GIP (1—42) and LPS stimulation (100 ng/mL) at the indicated time points. NFκB p65 activation was measured using the TransAM ELISA kit (Active Motif) according to the manufacturer's instructions.

RNA isolation and quantitative real-time reverse transcription-PCR: RNA was isolated using the RNeasy Mini Kit (74106; QIAGEN) and reverse transcribed using SuperScript III (18080-051; Invitrogen) according to the manufacturer's instructions. Quantitative real-time polymerase chain reaction analysis of target gene expression was performed using a ViiA7 Cycler (Applied Biosystems) and Sybr GreenER qPCR Super Mix for ABI Prism (11760-500; Invitrogen). Each sample was normalized to mRNA expression of the housekeeping gene ACTB.

Monocyte migration assay: Migration of RAW 264.7 cells and THP-1 cells (ATCC, USA) (human monocyte cell line) was determined as previously described [13]. Briefly, cells were cultured in serum-free media for 16 h. Monocytes (5×10^6 cells/ml) were pretreated for 30 min with GIP (1—42) at the concentrations indicated in serum-free medium and subsequently assayed for chemotaxis under serum-free conditions in a 48-well microchemotaxis chamber (Neuroprobe, UK). Wells in the upper and lower chamber were separated by a polyvinylpyrrolidone-free polycarbonate membrane (pore size 5 μm; Whatman, Germany). As a stimulus 10 nmol/l monocyte chemotactic protein-1 (MCP-1; PeproTech, USA) was added to the lower wells of the chamber. After 3 h, migrated cells attached to the bottom face of the filter were stained. Cells were counted under the light microscope in five random high-power fields per well as described [13].

Statistical analysis: Continuous data are presented as mean ± SD or SEM and median (Q1 — Q3) in case of skewed data. Categorical outcomes are shown as absolute and relative frequencies (%). For the experimental study, differences between groups were analyzed by one-way ANOVA, student's t-test or the Welch-Satterthwaite t-test. Post hoc tests were performed using the Holm-Bonferroni method. Linear regression analysis was performed in order to test for associations between plaque features. The GIP levels from the clinical study and the NFκB activation from the experimental study were compared using mixed models. Post hoc tests were conducted using Scheffe's method. Statistical analyses were performed with SPSS version 20 (IBM Corp., USA), SAS software version 9.4 (PROC GLIMMIX; SAS Institute, Cary NC, USA) or GraphPad Prism (USA). Statistical significance was intended for $p < 0.05$.

Table 2 — Multivariable Analysis: Mixed model for logarithmically transformed GIP-serum values.

	p-value	Estimate of log(GIP-serum) and 95%- confidence interval for CAD and PAD
Intercept	<.0001	5.5138
CAD	0.2287	0.1373 (No CAD), CI = (−0.08650, 0.3610)
PAD	***0.0411***	−0.2915 (No PAD), CI = (−0.5713, −0.01179)
Age	0.8232	0.000935
BMI	0.5253	0.005801
Sex	0.4632	0.05817 (female)
Hypertension	0.9850	−0.00213 (no hypertension)
DM	0.0549	−0.1466 (no DM)
CRP	0.6450	0.001337
WBC	0.7439	−0.00661
Smoker	0.1919	0.1351 (non-smoker)

Multivariable model with all covariates.
Bold represents significant association of GIP-serum levels and PAD with $p < 0.05$.

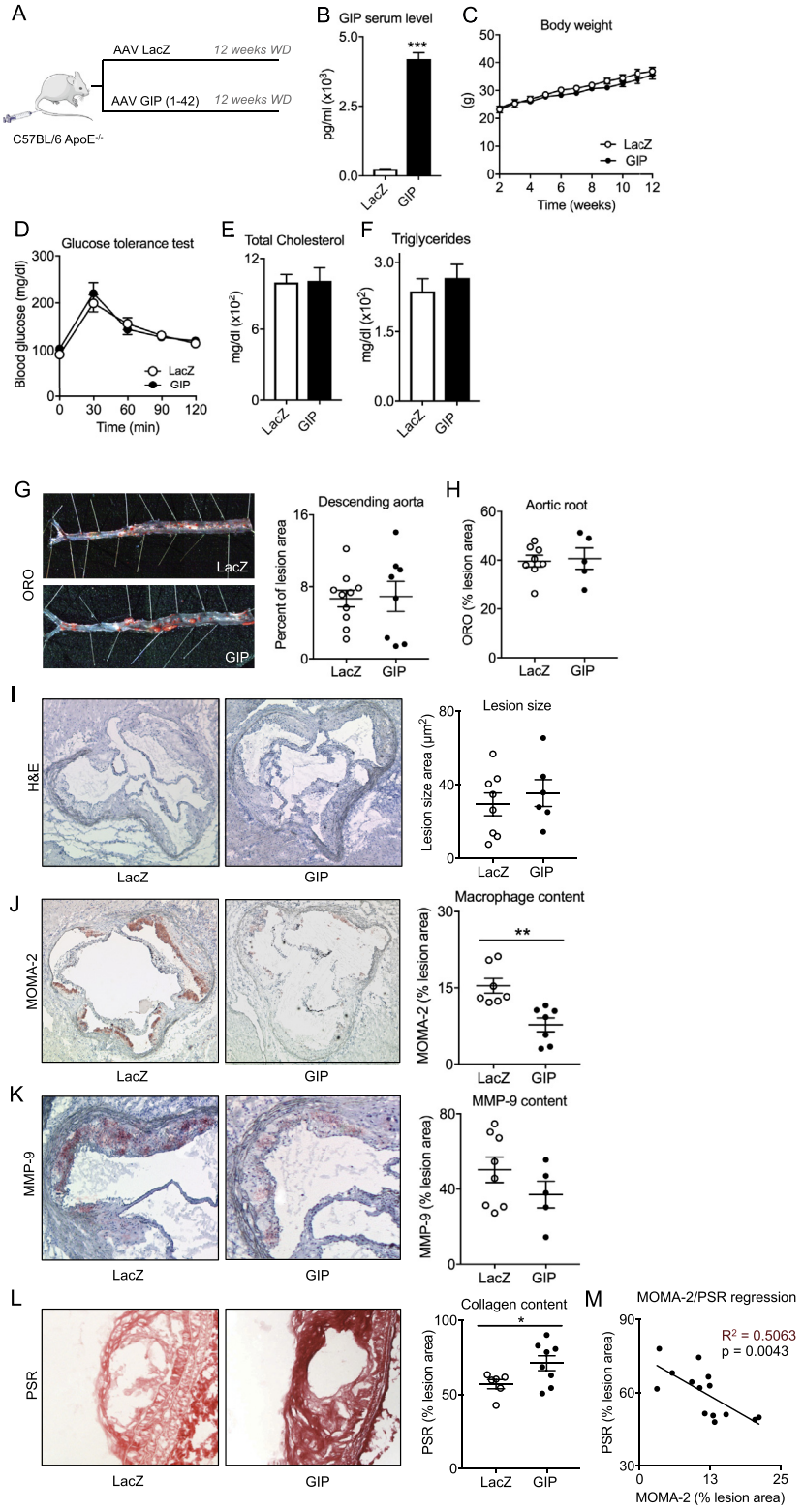

Figure 1: Analysis of atherosclerotic lesions in C57BL6 ApoE$^{-/-}$ mice after viral overexpression of GIP (1–42). Model to illustrate study protocol (A), serum total GIP concentrations 21 days after viral overexpression (B), body weight (C), oral glucose tolerance test 14 weeks after viral overexpression (D), final serum lipid measurement 16 weeks after viral overexpression (E, F) ($n = 5–10$). Results are expressed as the mean ± SEM. ***$p < 0.001$ vs. LacZ. Quantification of atherosclerotic plaque burden in the descending aorta (G) and the aortic root (H), representative pictures and respective quantification displayed by scatter plots of lesion extents visualized by H&E staining (I), macrophage content visualized by MOMA-2 staining (J), MMP-9 expression (K) and collagen content visualized by picrosirius red staining (L) in the aortic root (H–K) and aortic arch (L), linear regression analysis between plaque MOMA-2 expression and plaque collagen content (M) ($n = 5–10$). Results are expressed as the mean ± SEM. *$p < 0.05$ and **$p < 0.01$ vs. LacZ.

3. RESULTS

3.1. Patients with peripheral systemic atherosclerosis have elevated circulating GIP levels

To characterize the role of GIP in cardiovascular atherosclerotic disease, we first investigated circulating total GIP serum levels in patients who underwent elective coronary angiography at the University Hospital Aachen. GIP serum levels were not different in 474 patients with CAD (328.9 ± 285.8 pg/mL) vs. 257 patients without CAD (370.7 ± 314.9 pg/mL; $p = 0.1869$) (Table 1, Supplemental Table 1). Among the patients with CAD we also found no difference in GIP levels among those who required coronary intervention (319.9 ± 294.8 pg/mL) vs. patients without coronary intervention (331.4 ± 283.7 pg/mL) ($p = 0.3309$; Supplemental Table 2). Still, patients with PAD ($n = 97$) as a systemic manifestation of severe atherosclerotic disease presented with significantly higher circulating GIP levels (413.0 ± 315.3 vs. 332.7 ± 292.5 pg/mL) vs. 634 patients without PAD ($p = 0.0165$) (Table 1, Supplemental Table 1). This observation was similarly found in patients with CAD (391.2 ± 305.5 vs. 315.7 ± 280.1 pg/mL for 82 patients with vs. 392 without PAD; $p = 0.0389$), while there was a non-significant increase of GIP levels in patients without CAD (531.6 ± 352 vs. 360.5 ± 310.4 pg/mL for 15 patients with vs. 242 patients without PAD; $p = 0.0632$). The association between GIP levels and PAD remained significant in multivariable models after adjustment for age, sex, CAD, BMI (body mass index), hypertension, type 2 diabetes, CRP (C-reactive protein), WBC (white blood cell count), and smoking (Table 2). No association of GIP was found with age, BMI, sex, hypertension, type 2 diabetes, CRP, WBC, and smoking (Supplemental Table 1).

3.2. Viral overexpression of GIP in ApoE$^{-/-}$ mice

To investigate the functional relevance of elevated GIP levels in atherosclerotic disease we overexpressed GIP (1−42) and LacZ (control) in ApoE$^{-/-}$ mice fed a western diet for 12 weeks by using an adeno-associated viral vector system (Figure 1A). Compared to control (LacZ) viral overexpression of GIP (1−42) resulted in a significant elevation of serum peptide concentrations at day 21 after i.v. injection (Figure 1B) without affecting body weight, glucose tolerance, and serum lipids (Figure 1C−F).

3.3. Overexpression of GIP in ApoE$^{-/-}$ mice reduces plaque macrophage content without affecting lesion size

We next investigated the effect of GIP on atherosclerotic lesion size 12 weeks after initiation of Western diet. Compared to control GIP overexpression did not affect total lesion size and lipid content per plaque in the descending aorta and the aortic root and arch (Figure 1G−I, Figure S1). However, consistent with previous work by Nogi et al. [9], GIP significantly decreased macrophage plaque content as quantified by histological MOMA-2 staining (LacZ 15.4 ± 1.5% vs. GIP 7.8 ± 1.4% per lesion, $p = 0.002$) (Figure 1J).

3.4. Overexpression of GIP in ApoE$^{-/-}$ mice increases plaque collagen content

Given reduced macrophage content within the lesions by GIP overexpression we next analyzed characteristics of atherosclerotic plaque stability in these mice. We found a non-significant reduction of plaque specific expression of the macrophage-secreted matrix degrading enzyme MMP-9 (LacZ 50.2 ± 6.8% vs. GIP 37.1 ± 7.1% per lesion, $p = 0.228$) (Figure 1K). Picrosirius red staining was used to investigate the effect of GIP on plaque collagen content as an indicator of plaque stability. Significantly higher plaque collagen content was observed in the aortic arch and root of GIP treated mice (LacZ 57.0 ± 3.1% vs. GIP 71.1 ± 5.1% per lesion, $p = 0.016$) (Figure 1L and Figure S2). Taken into account the effects of GIP on plaque morphology we wondered whether the reduction in macrophage content was associated with increased collagen content per lesion by linear regression analysis. Indeed, high amounts of MOMA-2 expression significantly predicted low collagen content per lesion ($R^2 = 0.5063$, $p = 0.0043$) (Figure 1M), suggesting that GIP improves plaque stability by decreasing lesion macrophage content.

3.5. GIP inhibits chemokine-induced monocyte migration in vitro

Based on the GIP dependent reduction of atherosclerotic lesion macrophage content in ApoE$^{-/-}$ mice, we next questioned whether GIP directly affects monocyte migration. To this end, we performed In vitro migration assays using a modified Boyden chamber. As depicted in Figure 2A MCP-1 stimulated migration of murine (RAW 264.7 cells) or human monocytes (THP-1 cells) was blocked by pre-treatment with GIP at the indicated concentrations (Figure 2A). Mechanistically, we found GIP stimulation to reduce CCR2 expression in monocytes (Supplemental Figure S3) suggesting that GIP might reduce monocyte migration by directly inhibiting CCR2 surface expression.

3.6. GIP decreases macrophage MMP-9 production and enzymatic activity in vitro

With respect to our in vivo results of improved characteristics of plaque stability in GIP overexpressed mice, we next investigated if GIP has direct effects on MMP-9 production in endotoxin activated macrophages. Indeed, GIP treatment significantly prevented LPS-induced MMP-9 secretion (Figure 2B,C) and reduced MMP-9 enzymatic activity in murine macrophages, which is shown by using gelatin zymography (Figure 2B).

3.7. GIP blocks proinflammatory pathways in macrophages in vitro

Based on the inhibitory effect of GIP on atherosclerotic plaque inflammation and macrophage MMP-9 activity, we next elucidated the question whether GIP is able to attenuate intracellular proinflammatory pathways relevant for monocyte migration and MMP-9 expression. First, we stimulated RAW 264.7 cells with LPS for 24 h after pre-treatment with GIP at the indicated concentrations and measured IL-6 secretion to confirm whether GIP is able to functionally block proinflammatory cytokine production in macrophages. As depicted in Figure 2D GIP strongly inhibited LPS-induced IL-6 secretion in macrophages in a dose-dependent manner. To gain further mechanistic insights at the level of intracellular signal transduction we analyzed NF-κB activation as well as JNK, ERK and p38 signaling pathways. As shown in Figure 2E GIP treatment was able to prevent LPS-induced NF-κB activation 1 h and 2 h after LPS stimulation in RAW 264.7 cells. Furthermore, by using western blot analysis, we found GIP directly blocks activation of the proinflammatory MAPK (mitogen-activated protein kinases) family members JNK, ERK, and p38 in macrophages. LPS stimulation induced a strong phoshorylation of JNK, ERK and p38 after 30 min, which was prevented in the presence of GIP (Figure 2F−H), suggesting that GIP directly inhibits inflammatory activation of macrophages in vitro. Consistently, GIP overexpression in ApoE$^{-/-}$ mice significantly reduced hepatic expression of the proinflammatory cyto- and chemokines CCL5, IFN-γ, and IL-12 (while non-significantly inhibiting CCL2, TNF-α, and IL-6 expression), which are downstream targets of MAPK and NF-κB signaling (Supplemental Figure S4). These findings suggest that GIP mediated inhibition of monocyte/macrophage activation in vitro might translate into systemic anti-inflammatory effects in vivo in GIP overexpressed ApoE$^{-/-}$ mice.

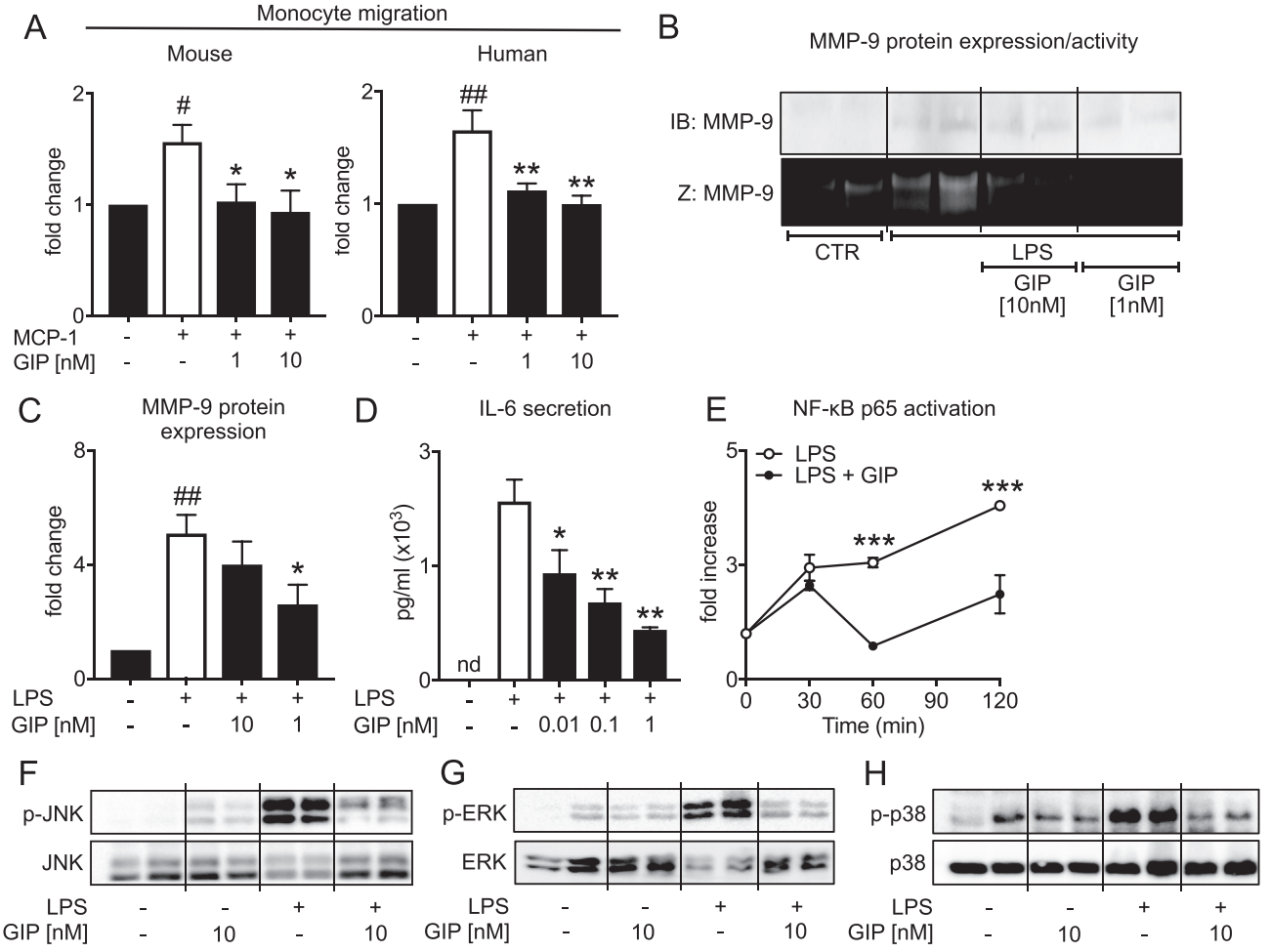

Figure 2: In vitro effects of GIP (1–42) on monocyte/macrophage inflammatory activation. Chemokine-induced migration of murine (RAW 264.7 cells) and human THP-1 monocytes. Monocytes were pretreated with GIP (1–42) for 30 min at the concentrations indicated before migration experiments using MCP-1 (10 nM) were performed in a modified Boyden chamber (A) ($n = 3–4$; $r = 4$), MMP-9 protein expression and activity analyzed by western blotting (IB) or zymography (Z) in the supernatant of RAW 264.7 cells 72 h after LPS stimulation (100 ng/mL) and 30 min pretreatment with GIP (1–42) at the indicated concentrations (B, C), IL-6 secretion of RAW 264.7 cells analyzed by ELISA 24 h after LPS stimulation (100 ng/mL) and 30 min pretreatment with 1 nM GIP (1–42) (D) ($n = 4$; $r = 3$), NF-κB p65 activation of RAW 264.7 cells at the indicated timepoints after LPS stimulation (100 ng/mL) and 30 min pretreatment with GIP (1–42) ($n = 2$; $r = 3$) (E) and western blot analysis of JNK, ERK, and p38 phosphorylation 30 min after LPS stimulation (100 ng/mL) and 30 min pretreatment with GIP (1–42) at the indicated concentrations ($n = 3$; $r = 2$). N: number of independent experiments; r: number of replicates. Results are expressed as the mean ± SEM. *$p < 0.05$, **$p < 0.01$ and ***$p < 0.001$ LPS/MCP-1 vs. LPS/MCP-1 + GIP, $^{\#}p < 0.05$, $^{\#\#}p < 0.01$ and $^{\#\#\#}p < 0.001$ LPS/MCP-1 vs. control.

4. DISCUSSION

In this study, we found circulating GIP concentrations to be elevated in patients with PAD as a manifestation of systemic atherosclerotic disease and identified GIP as a vasoprotective peptide stabilizing atherosclerotic lesions in ApoE−/− mice by preventing monocyte migration and blocking proinflammatory activation of macrophages. Given that plaque erosion and rupture are critical steps in the process of myocardial infarction, these findings might open new therapeutic avenues for patients with high cardiovascular risk.

Previous work by the Hirano group investigated the effect of GIP in murine atherosclerotic models and found infusion of GIP (1–42) by osmotic mini-pumps to decrease lesion size after 4 weeks in non-diabetic as well as in diabetic ApoE$^{-/-}$ mice [8, 9]. Mechanistically, the authors found GIP treatment to reduce plaque macrophage content and direct inhibitory effects on foam cell formation mediated via the GIP-receptor in diabetic ApoE$^{-/-}$ mice. However, it remains unclear whether GIP affects plaque morphology and stability and what is the underlying mechanism. Consistent with the previous study in diabetic ApoE$^{-/-}$ mice [9], we found a reduction in lesion macrophages after GIP overexpression in non-diabetic ApoE$^{-/-}$ mice. This effect could be mediated, in general, by a reduction in blood monocytes due to diminished myelopoiesis, changes in systemic or plaque cyto- and chemokine levels or altered chemokine receptor surface expression. Since recent work by Mantelmacher et al. found GIP to increase bone marrow hematopoiesis with the consequence of elevated numbers of differentiated blood leukocytes in mice [15], we speculate that changes in blood monocytes might not explain our phenotype. Here we found GIP to decrease hepatic proinflammatory cyto- and chemokine levels and to directly inhibit CCR2 expression in monocytes, which was linked to blocked MCP-1-induced monocyte migration In vitro. Based on these results, we speculate that both direct inhibition of CCR2 expression on monocytes as well as systemic (hepatic) reduction of cyto- and chemokine expression might contribute to GIP-mediated

reduction of plaque macrophages. However, compared to previous work [8, 9], we could not recapitulate a reduction of atherosclerotic lesion size by chronic GIP treatment, which might be attributable to different methodical approaches and treatment duration (osmotic mini-pumps and 4 weeks treatment vs. viral overexpression and 12 week treatment in our study). However, we demonstrated that GIP improves characteristics of plaque stability (reduced macrophage content and increased collagen content per lesion vs. control), which was linked to inhibitory effects of GIP on monocyte migration in vitro. The significant association between lesion macrophage and collagen content suggests that GIP might increase plaque stability by direct inhibition of plaque inflammation. Consistently, we found less MMP-9 production and a reduction of MMP-9 enzymatic activity after GIP treatment in macrophages In vitro. Mechanistically GIP non-selectively prevented endotoxin-induced activation of NF-κB, JNK, ERK, and p38 signaling pathways in macrophages. Future experimental studies are needed to better understand the exact molecular mechanism of GIP dependent modulation of proinflammatory pathways.

In the clinical part of the study we found a positive association between GIP serum levels and PAD as a manifestation of systemic atherosclerosis. In contrast, we did not find association of GIP with CAD. This might be explained by PAD being a strong indicator for advanced atherosclerotic disease, which is linked to worse prognosis relative to CAD patients [16]. These findings seem surprising given the vasoprotective effects of GIP in experimental atherosclerosis. Furthermore under physiological conditions GIP is secreted by intestinal K-cells [1] mainly following food intake. Since recent work demonstrated that GIP secretion can also be induced by inflammatory stimuli like IL-1, IL-6, and LPS independent from food intake [17, 18], we questioned whether the increase in GIP in our patient cohort was linked to inflammatory markers. However, we were unable to detect a significant association between GIP levels and the inflammatory markers CRP and WBC (Supplemental Table 1), making this an unlikely explanation. Interestingly, in a previous study by Nogi et al. [9], the authors found GIP-receptor mRNA expression to be reduced in diabetic vs. non-diabetic mice. Therefore, one might speculate that elevated GIP levels in patients with PAD are a result of reduced GIP-receptor expression in these patients, which will require further investigations. Additional studies are needed to clarify the underlying mechanism of elevated GIP levels in human systemic atherosclerosis.

5. CONCLUSION

By using a translational approach including a clinical study, mouse in vivo, and cell culture in vitro experiments, we here identified GIP as a previously unknown endogenous, couterregulatory, vasoprotective peptide that might open new therapeutic avenues for cardiovascular high risk patients with atherosclerosis. Future studies are warranted to determine whether these beneficial effects of GIP on features of plaque vulnerability and vascular inflammation translate in an improvement of cardiovascular outcomes in patients with type 2 diabetes at high cardiovascular risk.

ACKNOWLEDGMENT

This study was supported by grants from the Excellence Initiative of the German federal and state governments, the Else Kröner-Fresenius Foundation and the German Society for Cardiology (DGK) to F.K. and grants from the Deutsche Forschungsgemeinschaft (SFB TRR 219 M-03) and the Marga und Walter Boll-Stiftung, to M.L.

CONFLICT OF INTEREST

None.

APPENDIX A. SUPPLEMENTARY DATA

Supplementary data related to this article can be found at https://doi.org/10.1016/j.molmet.2018.05.014.

REFERENCES

[1] Baggio, L.L., Drucker, D.J., 2007. Biology of incretins: GLP-1 and GIP. Gastroenterology 132:2131–2157.
[2] Lehrke, M., Marx, N., 2012. New antidiabetic therapies: innovative strategies for an old problem. Current Opinion in Lipidology 23:569–575.
[3] Drucker, D.J., 2016. The cardiovascular biology of glucagon-like Peptide-1. Cell Metabolism 24:15–30.
[4] Burgmaier, M., Liberman, A., Mollmann, J., Kahles, F., Reith, S., Lebherz, C., et al., 2013. Glucagon-like peptide-1 (GLP-1) and its split products GLP-1(9-37) and GLP-1(28-37) stabilize atherosclerotic lesions in apoe(-)/(-) mice. Atherosclerosis 231:427–435.
[5] Arakawa, M., Mita, T., Azuma, K., Ebato, C., Goto, H., Nomiyama, T., et al., 2010. Inhibition of monocyte adhesion to endothelial cells and attenuation of atherosclerotic lesion by a glucagon-like peptide-1 receptor agonist, exendin-4. Diabetes 59:1030–1037.
[6] Marso, S.P., Bain, S.C., Consoli, A., Eliaschewitz, F.G., Jódar, E., Leiter, L.A., et al., 2016. Semaglutide and cardiovascular outcomes in patients with type 2 diabetes. New England Journal of Medicine 375:1834–1844.
[7] Marso, S.P., Daniels, G.H., Brown-Frandsen, K., Kristensen, P., Mann, J.F., Nauck, M.A., et al., 2016. Liraglutide and cardiovascular outcomes in type 2 diabetes. New England Journal of Medicine 375:311–322.
[8] Nagashima, M., Watanabe, T., Terasaki, M., Tomoyasu, M., Nohtomi, K., Kim-Kaneyama, J., et al., 2011. Native incretins prevent the development of atherosclerotic lesions in apolipoprotein E knockout mice. Diabetologia 54:2649–2659.
[9] Nogi, Y., Nagashima, M., Terasaki, M., Nohtomi, K., Watanabe, T., Hirano, T., 2012. Glucose-dependent insulinotropic polypeptide prevents the progression of macrophage-driven atherosclerosis in diabetic apolipoprotein E-null mice. PLoS One 7:e35683.
[10] Marso, S.P., House, J.A., Klauss, V., Lerman, A., Margolis, P., Leon, M.B., et al., 2010. Diabetes mellitus is associated with plaque classified as thin cap fibroatheroma: an intravascular ultrasound study. Diabetes and Vascular Disease Research 7:14–19.
[11] Milzi, A., Burgmaier, M., Burgmaier, K., Hellmich, M., Marx, N., Reith, S., 2017. Type 2 diabetes mellitus is associated with a lower fibrous cap thickness but has no impact on calcification morphology: an intracoronary optical coherence tomography study. Cardiovascular Diabetology 16:152.
[12] Lebherz, C., Gao, G., Louboutin, J.P., Millar, J., Rader, D., Wilson, J.M., 2004. Gene therapy with novel adeno-associated virus vectors substantially diminishes atherosclerosis in a murine model of familial hypercholesterolemia. The Journal of Gene Medicine 6:663–672.
[13] Vittone, F., Liberman, A., Vasic, D., Ostertag, R., Esser, M., Walcher, D., et al., 2012. Sitagliptin reduces plaque macrophage content and stabilises arteriosclerotic lesions in Apoe (-/-) mice. Diabetologia 55:2267–2275.
[14] Lehrke, M., Kahles, F., Makowska, A., Tilstam, P.V., Diebold, S., Marx, J., et al., 2015. PDE4 inhibition reduces neointima formation and inhibits VCAM-1 expression and histone methylation in an Epac-dependent manner. Journal of Molecular and Cellular Cardiology 81:23–33.
[15] Mantelmacher, F.D., Fishman, S., Cohen, K., Pasmanik Chor, M., Yamada, Y., Zvibel, I., et al., 2017. Glucose-dependent insulinotropic polypeptide receptor deficiency leads to impaired bone marrow hematopoiesis. The Journal of Immunology 198:3089–3098.

[16] Welten, G.M., Schouten, O., Hoeks, S.E., Chonchol, M., Vidakovic, R., van Domburg, R.T., et al., 2008. Long-term prognosis of patients with peripheral arterial disease: a comparison in patients with coronary artery disease. Journal of the American College of Cardiology 51:1588–1596.

[17] Kahles, F., Meyer, C., Diebold, S., Foldenauer, A.C., Stohr, R., Mollmann, J., et al., 2016. Glucose-dependent insulinotropic peptide secretion is induced by inflammatory stimuli in an interleukin-1-dependent manner in mice. Diabetes, Obesity and Metabolism 18:1147–1151.

[18] Ridker, P.M., Rifai, N., Stampfer, M.J., Hennekens, C.H., 2000. Plasma concentration of interleukin-6 and the risk of future myocardial infarction among apparently healthy men. Circulation 101:1767–1772.

